Journal of Nuclear Materials 386–388 (2009) 127–131

Contents lists available at ScienceDirect

Journal of Nuclear Materials

journal homepage: www.elsevier.com/locate/jnucmat

Damage to preheated tungsten targets after multiple plasma impacts simulating ITER ELMs

I.E. Garkusha [a,*], A.N. Bandura [a], O.V. Byrka [a], V.V. Chebotarev [a], I. Landman [b], V.A. Makhlaj [a]
S. Pestchanyi [b], V.I. Tereshin [a]

[a] Institute of Plasma Physics of the NSC KIPT, Akademicheskaya 1, 61108 Kharkov, Ukraine
[b] Forschungszentrum Karlsruhe, IHM, 76021 Karlsruhe, Germany

ARTICLE INFO

PACS:
52.40.Hf

ABSTRACT

The behavior of a preheated at 650 °C tungsten targets under repetitive ELM-like plasma pulses is studied in simulation experiments with the quasi-stationary plasma accelerator QSPA Kh-50. The targets have been exposed up to 350 pulses of the duration 0.25 ms and the surface heat loads either 0.45 MJ/m^2 or 0.75 MJ/m^2, which is below and above the melting threshold, respectively. The development of surface morphology of the exposed targets as well as cracking and swelling at the surface is discussed. First comparisons of obtained experimental results with corresponding numerical simulations of the code PEGASUS-3D are presented.

1. Introduction

In the future tokamak ITER, the divertor energy loads associated with the Type I ELMs are expected to reach $Q = 1–3$ MJ/m^2 during $\tau = 0.1–0.5$ ms, with the number of pulses per discharge about 10^3 [1]. The surface modification of divertor armor materials after the multiple impacts may cause significant changes of physical properties in a pre-surface layer and thus influence material behavior under the high loads. In ITER divertor design, tungsten is chosen as one of armor materials, however the brittleness of W gives rise to surface cracking [2]. To minimize the brittle destruction, the W-armor was suggested to be kept above the ductile-to-brittle transition temperature (DBTT) [3,4].

The energy density, the duration of ITER ELMs as well as particle loads can be well reproduced with quasi-steady-state plasma accelerators (QSPA). Cracking of the tungsten targets which had initially the room temperature (RT) has been investigated for ELM-like plasma loads below melting threshold, in conditions of pronounced melting and with achieving the evaporation threshold correspondingly [5–7]. With increasing the number of exposures significant threshold changes in surface morphology have been observed. First results of preheated tungsten exposures by repetitive ELM-like plasma loads at the QSPA Kh-50 [5,7] and the QSPA-T [8] also showed contribution of cracking to the tungsten damage, despite the total number of pulses has not exceeded 100, which is much less than expected in one ITER discharge. Thus, the behavior of preheated W-surface under pulsed plasma loads typical of transient events in ITER requires further comprehensive experimental studies with larger numbers of exposures. In this work the W-targets underwent up to 350 plasma shots and this experiment is described, discussed and compared with dedicated numerical simulations.

2. Experimental setup

The repetitive plasma exposures have been performed using the QSPA Kh-50 [9–11]. Tungsten targets of EU trademark have the sizes $5 \times 5 \times 1$ cm. A molybdenum diaphragm with a hole of 3 cm was used to protect the target edges from the plasma impact, to provide the reference line for profilometry measurements, and also to simulate the case when the target sizes exceed the diameter of plasma stream. An electric heater was installed at target's backside to keep the target temperature of 650 °C before each plasma pulse. For temperature monitoring a calibrated thermocouple and an infrared pyrometer were used. All the targets were exposed to perpendicular plasma irradiation. The main parameters of hydrogen plasma streams are as follows: ion impact energy about 0.4 keV, maximum plasma pressure 3.2 bar, and the plasma stream diameter 18 cm. The surface energy load measured with a calorimeter was either 0.45, which is below the melting threshold, or 0.75 MJ/m^2, which is between the melting- and evaporation thresholds. The plasma pulse shape is approximately triangular, pulse duration of 0.25 ms.

* Corresponding author.
E-mail address: garkusha@ipp.kharkov.ua (I.E. Garkusha).

0022-3115/$ - see front matter © 2009 Published by Elsevier B.V.
doi:10.1016/j.jnucmat.2008.12.083

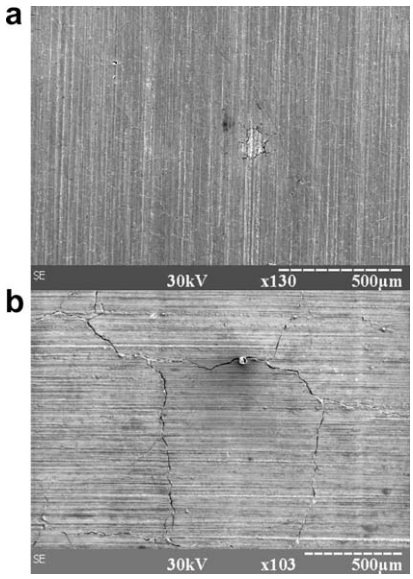

Fig. 1. Tungsten surface after 210 plasma pulses of 0.45 MJ/m^2: (a) preheated target 650 °C, (b) RT target.

3. Experimental results

3.1. Tungsten exposure with repetitive pulses below the melting threshold

In the experiments below the melting point the W-target was exposed to 210 plasma pulses of the energy density 0.45 MJ/m^2. The surface morphology changes were analyzed with optical microscopy and SEM by monitoring the same surface regions after different number of pulses.

It is revealed that macro-cracks are completely absent on the preheated surface (Fig. 1(a)). For comparison, after similar exposures of W-target at the room temperature the mesh of macro-cracks with mean cell size of 0.5–1 mm is clearly seen (Fig. 1(b)). No cracks at all were registered on the preheated surface in result of several tens pulses. After first hundred of plasma pulses only some micro-cracks were found. It is concluded that they are fatigue cracks as the result of repetitive stresses induced by numerous plasma impacts (Fig. 2). This observation is in agreement with [8] where the cracks on resolidified surface were also formed after definite number of exposures. However, the macro-crack network with the cell sizes of ~0.5–1 mm observed in [8] is not registered in our experiments for the target preheated at 650 C. Initially arisen separate cracks do not form a mesh on the surface. Only after 200 exposures a completed mesh of cracks became clearly seen, with the mesh sizes varying in the range of 20–70 μm and the crack width less or about micron. While the main target surface remains not molten in the course of repetitive pulses, the edges of cracks became to melt, which is attributed to decreased heat transfer from the edges.

Fig. 2 demonstrates fatigue cracks after 100 (a, b) and 150 (c) pulses. Development of cracks obviously leads to local deterioration of the heat conductivity in cracked volume. The corresponding surface modification under following plasma pulses occurs due to the local overheating of the surface areas pre-damaged by cracks. It can be caused by fast quenching of thin surface layer in the conditions with large temperature gradient of order of 10^6 K/cm. Surface modification results in formation of submicron or nano-cellular structures, which are shown in Fig. 3 with different magnifications. The sizes of cellular structure up to 500 nm are much less than initial size of tungsten grains. Similar morphology on nano-scale was described in [7] after W-target exposures to plasma loads above the melting point. It is also to notice that cellular structures of submicron- and nano-size were found, too, after exposures of W-target to e-beam impacts [12].

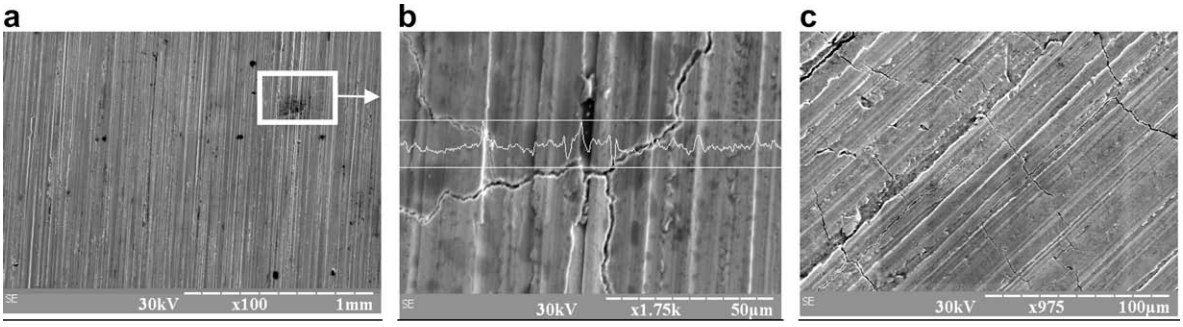

Fig. 2. Development of cracks on the tungsten surface in result of plasma exposures below the melting threshold. Surface heat load Q = 0.45 MJ/m^2.

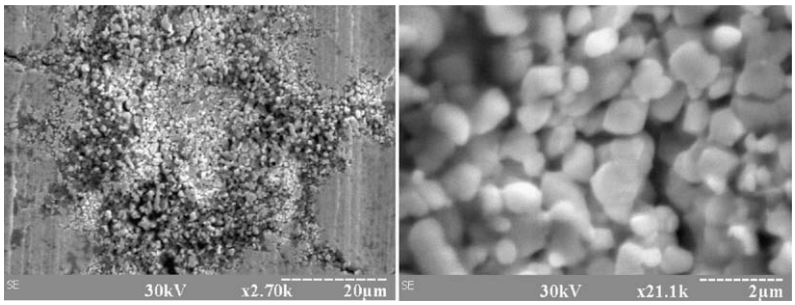

Fig. 3. Morphology of exposed tungsten surface under different magnification after 210 plasma pulses of 0.45 MJ/m^2.

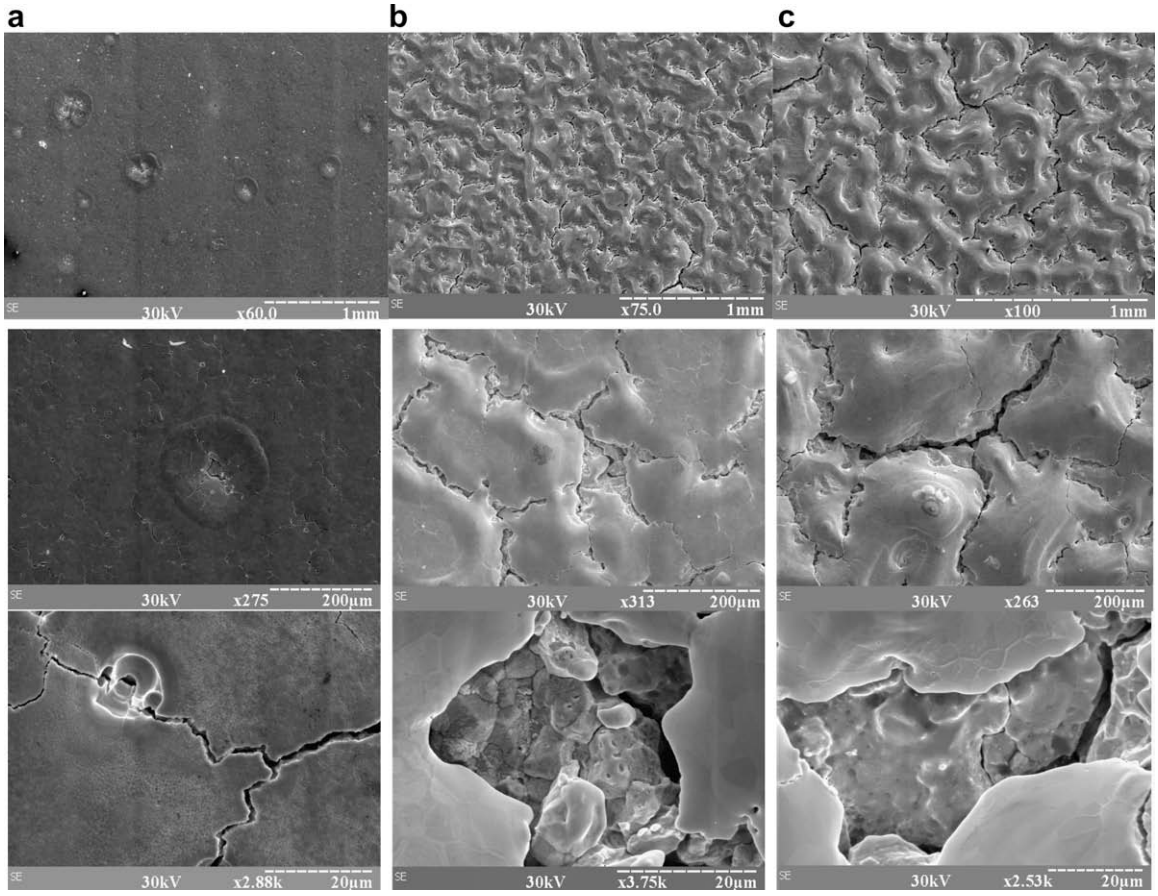

Fig. 4. SEM images of the tungsten surface after 100 (a), 210 (b) and 350 (c) pulses (Q = 0.75 MJ/m^2) with different magnification.

The morphology patterns look like 'foam plastic' structures that have arisen on different areas of the exposed surface. With increasing the number of exposures the number such regions and their areas are growing. Further pulses result in the melting onset of modified regions whereas other surface remains non-melted. Thus, surface modification may cause changes of physical properties of the surface layer and thus influences the material behavior under the high plasma heat loads [13]. It should be mentioned that pronounced degradation of thermal conductivity due to the cracking process was observed as result of targets exposures at room temperature [5]. Surface melting was achieved after 170 pulses of the same heat load of 0.45 MJ/m^2.

3.2. Tungsten exposures above the melting threshold

Fig. 4 demonstrates the damage to preheated tungsten surface after multiple pulsed loads of 0.75 MJ/m^2 that cause surface melting. Microscopy observations show that the surface remains rather stable with increasing number of exposures up to 100–130 pulses. However, after 100 pulses blisters and bubbles with the size of 100–300 μm develop [7]. Inside blister voids and in crack volumes some balls of the sizes of 10^{-2}–1 μm are seen (Fig. 5(b) and (c)). In addition, cellular submicron structures develop. Blisters do not contribute significantly to the total erosion and they disappear with increase of the exposition dose.

The most important changes in surface morphology are observed increasing the pulse number above 200. This resulted in qualitative evolution of the surface morphology. The surface became similar to that observed earlier [5,6] for 200 exposures of RT targets with the same energy load (0.75 MJ/m^2) and with the energy load of 1.1 MJ/m^2, which corresponds to the evaporation threshold. The obtained results prove that threshold changes of surface morphology are practically the same for all mentioned cases.

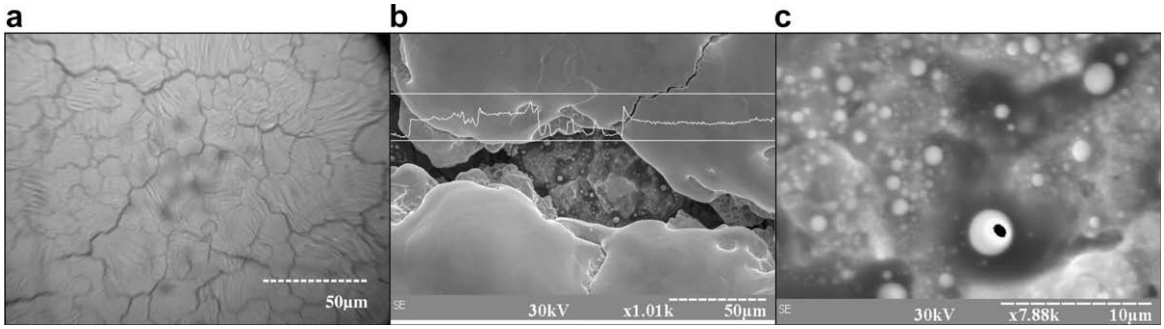

Fig. 5. Cracks on the tungsten surface after 80 and 310 plasma pulses of 0.75 MJ/m^2 (a, b). Enlarged view of nano-balls in the crack void (c).

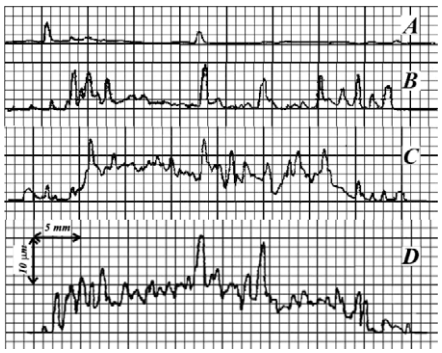

Fig. 6. Evolution of surface profiles of preheated tungsten in the course of plasma exposures: (a) 80 pulses, (b) 150 pulses, (c) 210 pulses, (d) 350 pulses of 0.75 MJ/m^2.

Due to the corrugations, the initially uniform melt layer tends to be transformed into 'shagreen leather' (Fig. 4(b)). Such evolution is sequence of the surface cracking. A fine mesh of intergranular cracks becomes well seen already after 25 exposures. During each pulse the meshes melt and after the pulse new crack network appears. With increasing the pulse number the crack width gradually increases, getting of 0.8–1.5 μm after 100 pulses and up to 20 μm after 200 pulses. Due to intergranular cracks, surface areas of 20–50 μm become separated from each other by the cracks forming an ensemble of micro-brushes. The melting at next pulses does no longer result in mixing because of the increased depth and width of the cracks and negligible melt motion on small brush surface. Being separated, each cell of the cracks network is strongly subjected to the surface tension that minimizes cell area. As the result, after the large number of exposures the progressive corrugation of the surface develops. Fig. 5(a) demonstrates the enlarged view of cracks and appeared strips on resolidified surface as 'footprints' of surface tension action. Further evolution of the surface pattern with increased number of impacts is caused by removal of W-grains from the eroded surface. After 350 pulses the surface becomes extremely destroyed by the cracks in spite of preheating (Fig. 4(c)).

The microscopy observations well correlate with profile measurements. The profile swelling starts after 200 pulses as result of threshold changes in surface morphology (Fig. 6).

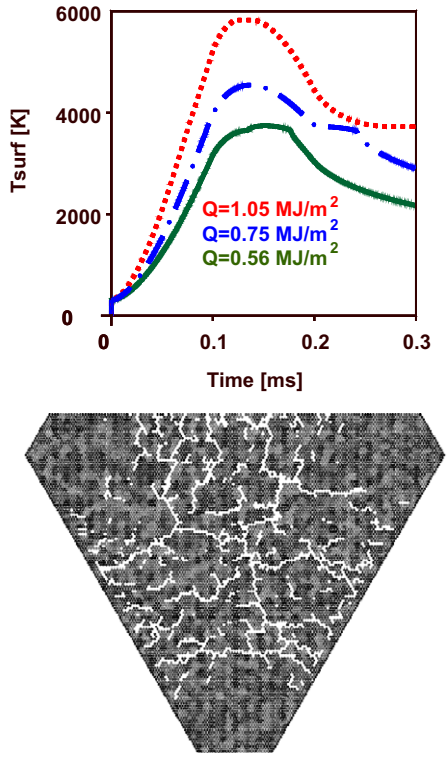

Fig. 7. Calculated surface temperature during the plasma pulse and result of the PEGASUS-3D simulation of the cracks developed in tungsten sample after irradiation.

4. Numerical simulation results

For theoretical interpretation of tungsten damage after irradiation with hydrogen plasma of QSPA Kh-50 numerical simulation has been performed using the code PEGASUS-3D described elsewhere [14]. As the time dependence for heat flux to the sample surface the triangle pulse shape was assumed. For tungsten thermophysical parameters the reference temperature dependences from [15] have been used.

At first the melting threshold 0.56 MJ/m^2 and the vaporization threshold 1.1 MJ/m^2 measured under the QSPA Kh-50 heating conditions for the undamaged tungsten samples have been reproduced in the simulation. Indeed, using for fitting at any temperature the reduction coefficient 0.9 at the reference thermal conductivity the melting threshold 0.58 MJ/m^2 for the energy absorbed by the target and the vaporization threshold 1.05 MJ/m^2 have been calculated (Fig. 7). Additional information on the tungsten thermal conductivity was obtained from the plasma shots with the heat load 0.75 MJ/m^2. With the same reduction coefficient of 0.9 the simulated melt layer thickness is 17 μm, to be compared with that of 15 μm directly measured in the experiment. The necessity of fitting is attributed to the accuracy of measurements of power density profile and to the tungsten surface damage by cracks during few tens of plasma shots needed for the threshold measurements.

In addition a numerical simulation with PEGASUS-3D of tungsten surface cracking under the thermal stresses in thin resolidified surface layer was performed. First simulation results qualitatively reproduce experimental pattern of cracks on the surface (Fig. 7) and characteristic scales of crack meshes in cases of plasma exposures in the conditions of surface melting.

5. Conclusions

The behavior of preheated tungsten targets under repetitive ITER ELM-like plasma pulses is studied in the tokamak simulation experiments at the quasi-stationary plasma accelerator QSPA Kh-50. Comparisons of surface damages after multiple heat loads both below and above the melting threshold are performed.

Target preheating above DBTT allows suppressing the formation of macro-cracks on W-surface. After first hundred of plasma pulses only micro-cracks were found and it can be classified as fatigue cracks resulting from repetitive stresses induced by numerous plasma impacts. Surface modification with formation of ordered submicron or nano-cellular structures was observed. The balls of nm size were registered inside the crack volumes. The importance of cellular structures arisen for estimation of material response to the ITER transient events is demonstrated.

After several hundreds of exposures the damage caused by cracking becomes dominant. Thus, tungsten cracking cannot be completely mitigated by the preheating above the DBTT. However, the damage can be significantly minimized, especially at the irradiation below the melting threshold.

For the preheated target with the surface melting loads the surface cracking is accompanied by the swelling which demonstrates the influence of surface tension resulted from the formation of 'micro-brush' structures similar to the W-targets exposed at the room temperature.

First comparison of experiments with numerical simulation showed that the applied code PEGASUS-3D qualitatively reproduces the crack pattern on the resolidified surface.

The influence of cracks on degradation of thermal conductivity in a thin pre-surface layer after large numbers of exposures can be important for ITER operation. Therefore more detailed both experimental and theoretical studies of surface cracking mechanisms below the melting threshold and the influence of preheating on the erosion processes are required.

Acknowledgment

This work has been supported in part by STCU project #4155.

References

[1] G. Federici et al., Plasma Phys. Control. Fus. 45 (2003) 523.
[2] J. Linke, G. Pintsuk, M. Roedig, A. Loarte, Performance of plasma facing materials under repeated ELM loads, Proceedings of the International Conference on Fusion Reactor Materials, 10-14 December 2007, Nice, France on CD-ROM, p. 55.
[3] S.W.H. Yih, C.T. Wang, Tungsten: Sources, Metallurgy, Properties and Application, Plenum Press, NY and London, 1979.
[4] G. Federici et al., Nucl. Fus. 41 (2001) 967.
[5] I.E. Garkusha et al., J. Nucl. Mater. 337–339 (2005) 707.
[6] V.I. Tereshin et al., Plasma Phys. Control. Fus. 49 (2007) A231.
[7] V.A. Makhlay et al., Phys. Scr. 128 (2007) 239.
[8] A. Zhitlukhin et al., J. Nucl. Mater. 363–365 (2007) 301.
[9] V.I. Tereshin, Plasma Phys. Control. Fus. 37 (1995) A177.
[10] A.I. Morozov et al., Plasma Dev. Oper. 2 (1992) 155.
[11] V.I. Tereshin et al., J. Nucl. Mater. 313–316 (2003) 685.
[12] J. Linke, G. Pintsuk, private communication.
[13] N. Ohno, S. Kajita, Dai Nishijima, S. Takamura, J. Nucl. Mater. 363–365 (2007) 1153.
[14] S. Pestchanyi, H. Wuerz, Phys. Scr. T91 (2001) 84.
[15] Y.S. Touloukian (Ed.), Thermophysical Properties of High Temperature Solid Materials, vol. 1: Elements, The Macmillan company, New York, 1967.